Measurement of the point spread function in the ocean

Kenneth J. Voss and Albert L. Chapin

A new instrument to measure the point spread function (PSF) in the ocean is described. This instrument uses a CCD solid state camera to measure the angular radiance field due to a pulsed Lambertian source. In this way the PSF can be measured easily at sea, when precise alignments over ranges >10 m cannot be maintained. With the large dynamic range of the camera system, the PSF can be measured over short ranges (10 m), and the variation of the PSF with depth, or range, can be investigated. *Keywords*: Ocean optics, point spread function, light scattering, image transmission.

I. Introduction

The point spread function (PSF) is an important parameter in modeling imaging properties in seawater and may be an important function for characterizing the small angle scattering phase function and particulate size distribution. The PSF has been used in characterizing lenses,[1] imaging in the atmosphere,[2] and to some extent imaging of seawater.[3] Very few measurements of the PSF for seawater exist in the literature, and the variability of the parameter is unknown. A new camera system has been built to measure the PSF in seawater, determine the variability of this parameter, and investigate theories relating the PSF to the small angle scattering function. This instrument, based on a cooled CCD array camera, allows rapid measurement of the PSF in two modes: (1) constant range and variable depth (to sample the water column) and (2) variable range. The camera system is described, calibration of the system is detailed, and a sample data set is presented.

II. Definitions and Theory

The best definition of the PSF is given by Mertens and Replogle.[4] In this paper they define the PSF (θ,ϕ,R) as the apparent radiance of an unresolved Lambertian source at the position $(0,0,R)$ normalized to source intensity. This quantity has units of m^{-2}. In a more physically intuitive but less mathematically and photometrically correct terminology, the PSF for a given range is the blurred image of a point source at a range R. In the case of no scattering, the PSF is a delta function in the center of the image. With scattering, the image of the point source is blurred, and this blurring is a measure of the PSF. In these measurements, the source is not actually a point source but rather a Lambertian source with dimensions that are small compared to the resolution of the receiver. The measurement obtained with this Lambertian source allows the image of any object (assuming a Lambertian surface for this object) to be predicted by modeling the surface with a collection of these point sources. It is for this reason that the PSF is such a valuable parameter for image predictions. Mertens and Replogle[4] showed that the beam spread function (BSF), the spreading of a light beam due to scattering, is mathematically equivalent to the PSF. Thus the PSF can also be used in predicting the propagation of collimated light in the ocean.

It is also important to investigate how the PSF is related to the small angle scattering function. Wells[5] showed theoretically that the PSF could be linked to the scattering function for the case of unpolarized light in the small angle limit. This derivation linked the PSF, modulation transfer function (MTF), and scattering phase function in the following manner: the PSF(θ,ϕ,R) is the 2-D Fourier transform of the MTF, or, since the PSF is rotationally symmetric [PSF(θ,ϕ,R) is independent of ϕ], PSF(θ,R) is the Fourier-Bessel transform of the MTF.

The MTF is then related to the scattering phase function by

$$\mathrm{MTF}(\psi,R) = \exp[-D(\psi)R],$$

where $D(\psi) = c - \Sigma(\psi)$; here $\Sigma(\psi)$ is the Fourier-Bessel transform of the scattering phase function, c is the beam attenuation coefficient, and ψ is the angular frequency. Physically, $\Sigma(\psi)$ corresponds to a restoring function for the attenuation coefficient at low angular frequencies. $\Sigma(\psi)$ goes to 0 at high frequencies, while at low frequencies $\Sigma(\psi)$ goes to b_{forward}, the forward component of the scattering coefficient. This implies that $\exp(-KR) \rangle= \mathrm{MTF}(\psi,R) \rangle= \exp(-cR)$, where K is the diffuse attenuation coefficient. These

theories enable one to calculate the PSF given the volume scattering function (including the very small angle component), or, given the PSF, one can invert these equations to find the small angle volume scattering function. However, this derivation is based on a small angle approximation, and experimental verification of these approximations is necessary.

The small angle scattering function of seawater itself can be related to the size distribution of the particulates in the seawater. The scattering function of seawater is very sharply peaked in the forward direction. This small angle scattering is predominantly dependent on the size distribution of the particulates. In this region, the predominant mode of scattering is through diffraction; hence the index of refraction is not important.[6] Morel, in extensive computations of Mie scattering functions for collections of spheres with Junge type size distributions, found that the slope of the scattering function could be related to the exponent in the size distribution.[7] This can be expressed by the following formula:

$$m = \frac{\theta d\sigma}{\sigma d\theta} \, ,$$

where $N(D) = AD^{-m}$ and θ is the scattering angle, $\sigma(\theta)$ is the light scattering phase function, N is the size distribution function, D is the diameter of the particles, and A is a constant. With this information, a method of measuring the size distribution of the oceanic particulates *in situ* can be developed through use of the PSF. This method depends heavily on the theories derived by Wells; thus a major goal of the planned deployment of this instrument is in determining the validity of these theories.

III. Instrumentation

Methods used to measure the PSF, or BSF, previously have involved the use of either large water tanks[8] or a large underwater track system.[4] The first method suffers from the obvious drawback of not being an *in situ* measurement, thus limiting its use in exploring the effects of structure in the water column. The second method is cumbersome if measurements are desired in varied water types and conditions. The method we have selected, first developed by Honey,[9] involves using a point source (a flashlamp) and an imaging camera system. The camera system is based on a cooled charge coupled device (CCD) camera (Photometrics, Ltd., model CC-200) and controller (Photometrics, Ltd., model CE-200). The CCD array (576 × 384 pixels, Thompson CSF TH7882CDA) is thermoelectrically cooled to allow the array to have very low noise rates (of the order of 10 thermally generated electrons per pixel) and a large dynamic range due to the large electron well depth ($\sim$2.5 × 10^5 electrons/well). There are several important features of the camera housing assembly. First, the camera is mounted in the case and held in place with aluminum rings which serve as thermally conductive paths to the outside case. In this manner the heat which has been removed from the array is conducted to the case, and

the ocean water is used as a heat sink. The camera lens used in this case is a bayonet mounted 24-mm lens (standard 35-mm format camera lens, Tamron *f2.5*). This lens is focused at infinity so that the image obtained with the camera is a map of the angular radiance field at the location of the instrument. (Each pixel collects the light from a given θ and ϕ.) An interference filter is placed in front of the lens to allow selection of the spectral band of interest, and a flat plate window is used as the viewpoint. This window is coated on the interior side with an antireflection coating but has no coating on the exterior surface relying on the index matching characteristics of the water. A flat window does not change the imaging characterisitcs of the lens with the lens focused at infinity. However, the air–glass–water interface must be taken into account when geometrically calibrating the lens mapping function. While a spherical window allows larger angles to be sampled (the field is not reduced by the interface refraction), one can have problems unambiguously mapping the pixel location with its angular field. The camera electronics are placed in an area behind the camera. The CCD is read using a 14-bit A–D converter which takes advantage of the intrinsic dynamic range of the camera. This dynamic range allows measurement of the PSF over short ranges. The image data are digitized and then transmitted up a multiconductor cable to the deck controller and then to an HP-332 computer. The computer can display the image, store the image on a 6.35-mm (0.25-in.) tape or disk, and process the image to obtain the PSF. A pressure transducer located on the faceplate of the camera provides the camera depth used in determining the range.

The light source is a xenon flashlamp with a diffuser to approximate a Lambertian source. The flashlamp (compact bulb type flashlamp EG&G 5M-3), power supply (EG&G PS-450), and flashlamp capacitor (30 μF,1 kV) are all contained in the flashlamp housing. The power for the flashlamp unit is multiplexed with the signal from the pressure transducer, and the trigger signal for the flashlamp is carried on a separate conductor. A BK7 window placed between the diffuser and flashlamp serves as the watertight element for the housing. This allows the diffuser to be changed without affecting the watertight housing. The design of the cosine emitter is similar to that of a cosine collector,[10] and the emission characteristics are described in Sec. IV.

These two pieces can be arranged in two configurations. The first is with the camera remaining just below the surface of the water and varying the depth of the light source. In this method the variation of the PSF with distance, or R, can be investigated. The second configuration is to set the camera and light source a fixed distance apart and vary the overall depth of the system. In this way the system measures the profile of the PSF through the upper portion of the water column. The minimum range which can be measured in clear water is $\sim$10 m with the system as designed.

IV. Calibration

A. Camera

There are several calibration steps for both the camera and flashlamp which are crucial to understanding the measurement. Camera linearity was tested by viewing the center of a radiance reflectance plaque with the camera and varying the position between the plaque and a calibrated standard lamp. The irradiance incident on the plaque, hence the radiance from the plaque, can be calculated from the lamp calibration values and the inverse square law. A portion in the center of the plaque is averaged for each image obtained. The camera was found to be linear over a 50-dB range when averaging can be used to extend the low end below 1 count. Thus the 14 bits of digitization are appropriate for this camera system.

Moving out from the array, the next step is a geometric calibration of the lens system. This is done by simply placing the camera 3 m from a point source and accurately rotating the camera with respect to the point source. The function mapping array position with angular space should be a sine function and was found to be quite well described (regression coefficient was >0.999) by the function

$$\theta(\deg) = \arcsin(0.947\#).$$

The $\#$ represents the radius from the center of the array in pixels. When using the camera in the field, this equation must be modified to account for the refraction at the air–glass–water interfaces. The equation then becomes

$$\theta_w(\deg) = \arcsin(0.947\#/n_w),$$

where n_w is the index of refraction of the water (~1.34).[11] The PSF of the camera must also be measured to determine the minimum measurable PSF of the instrument system. Figure 1 illustrates the PSF vs angle for seawater at 10 m (measured with the system in Tongue of the Ocean, Bahamas, a very clear water station) and the measured PSF of a small source in air at various angles through the lens. In air the PSF is assumed to be due totally to the camera system. As can be seen, the PSF of the camera–lens–window system is very small even when compared with the PSF of clear seawater at small range. Thus this camera PSF can be neglected in the field measurements.

The camera system rolloff is also an important parameter and must be taken into account in the data reduction process. The calibration factor for the rolloff is measured by filling the field with a uniform source of radiance. The image obtained is normalized to the value at the center of the array and inverted to form a calibration image. Each data image, during the data reduction process, is multiplied pixel by pixel with this calibration image, thus correcting for camera lens rolloff effects.

Last, for the camera assembly, the spectral response of the camera, lens, and filter system must be determined. This is done by viewing a small reflectance
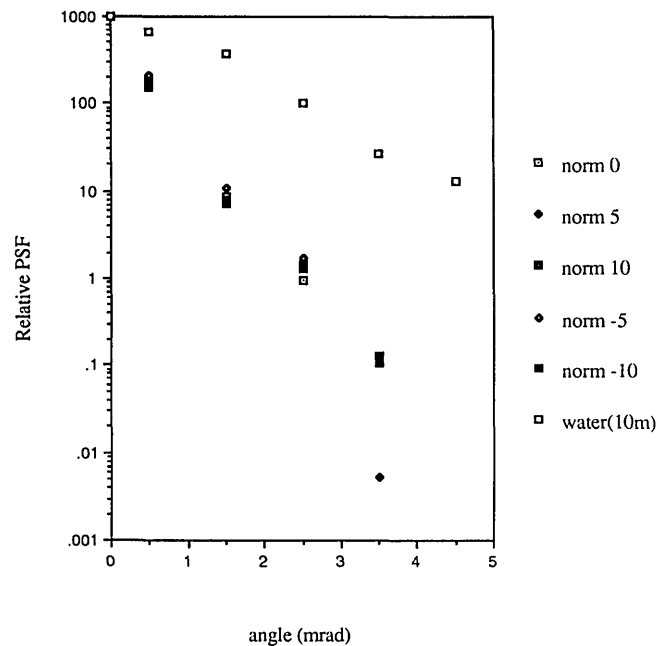

Fig. 1. PSF vs angle for clear water and a small source in air. The water symbol is shown. Other symbols correspond to imaging through different angles of the camera (norm 0 is at 0°, etc.). The PSF for the camera is constant with angle, negligible compared with clean water, and thus can be neglected in the data reduction process.

plaque, which is illuminated by monochromatic flux, with the camera (including lens and filter). The spectral characteristics of this system are shown in Fig. 2. The spectral bandpass of the system was at 501.5 nm with a 10.0-nm bandwidth. These characteristics are measured with the camera system normal to the
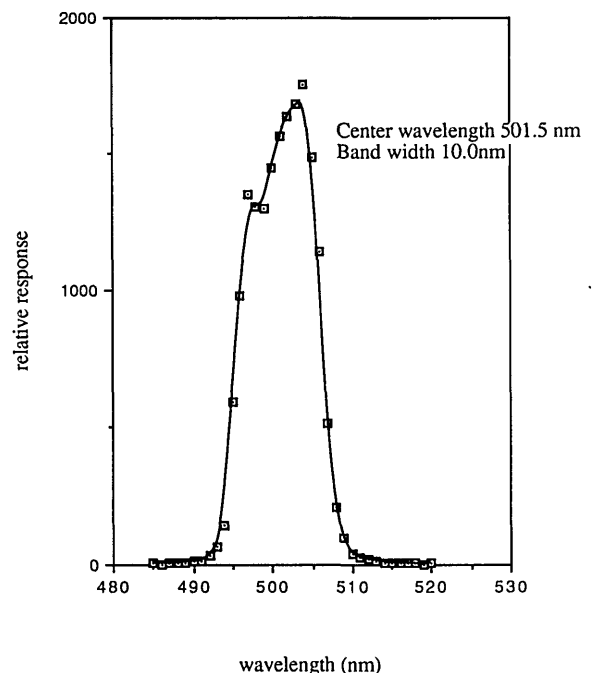

Fig. 2. Spectral response of camera and filter combination.

plaque; thus the monochromatic flux was normal to the interference filter. Some shifting of the central bandpass can be expected toward the edge of the image due to light rays striking the interference filter at oblique angles. However, this effect causes only a small change in bandpass and a negligible change in the PSF.

B. Flashlamp

There are two steps to the flashlamp calibration: (1) energy distribution of emitter; (2) pulse-to-pulse variability. The energy output of the flashlamp was measured by placing the camera 2 m from the flashlamp in a tank filled with filtered water. The pulse energy collected by the camera from the angular area subtended by the flashlamp was integrated. The flashlamp was rotated about an axis located on the front of the cosine emitter, and several measurements were obtained and averaged for each angle to reduce the effect of pulse-to-pulse variations. The results of this calibration step are shown in Fig. 3 where it can be seen that the emission follows the intended cosine function quite well.

The pulse-to-pulse variability was determined by repeatedly triggering the flashlamp and measuring the average output with the camera. It was found that the flashlamp pulse energy was constant to within 6% standard deviation.

V. Data

Once an image is obtained, the steps to determine the PSF are quite simple. Because of radial symmetry, the PSF is obtained by taking a radial average around the image of the source. Several example PSFs are shown in Fig. 4. These measurements were performed in Tongue of the Ocean, Bahamas on 5 Mar. 1989 from the USNS Bartlett. For each of the PSFs illustrated, the camera was at a depth of 1 m, while the separation of the camera and flashlamp varied from 11.2 to 27.0 m. This illustrates two aspects of the data obtained with this instrument. First, the emitter subtends ~2 mrad at a distance of 11 m (emitter is 55 mm in diameter) and ~1 mrad at 27 m. Thus this central portion is the direct radiance from the source, including scattering of <2 mrad and any multiple scattering which causes light to reenter the path. This central portion of the image can be used to measure the beam attenuation with very fine angular resolution and over a large water path. Second, at ~4 mrad in the short range case, the true PSF begins. At this point the trend toward decreasing slope with increased range can be observed.

The water column, over which the above measurements took place, was homogeneous, as evidenced by Fig. 5 in which the PSF for a fixed range and varied depths are plotted. These data were taken at approximately the same time (within an hour) and location as in Fig. 4. The range for each of the measurements is 13 m, with the camera depths (the top end of the range) at 1.0, 12.0, and 22.3 m. As can be seen, the PSF was very constant over this region with significant changes in
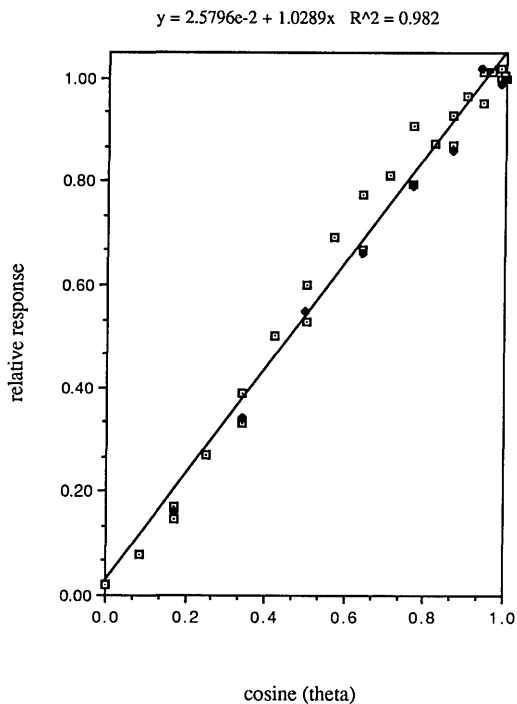

$y = 2.5796e-2 + 1.0289x \quad R^2 = 0.982$

Fig. 3. Emission characteristics of the flashlamp emitter. The emitter does perform as a cosine source.

A) 11.2m range
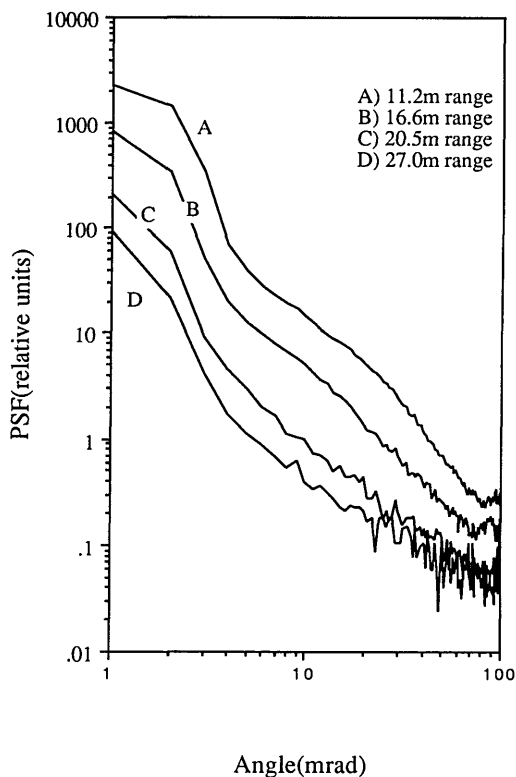B) 16.6m range
C) 20.5m range
D) 27.0m range

Fig. 4. PSF vs angle for various ranges. In all cases the camera was held at a depth of 1.0 m. These data were taken in Tongue of the Ocean, Bahamas, in clear water. Data show the general decrease in received radiance with increased range along with a flattening of the PSF with increased range.
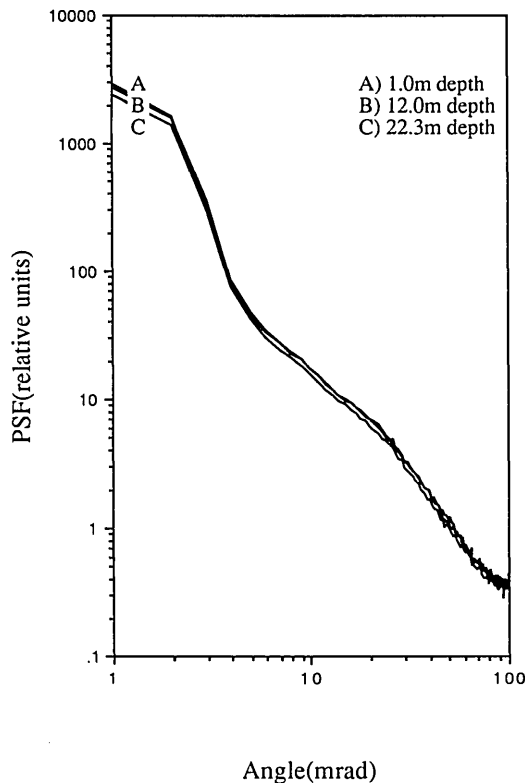
Fig. 5. PSF vs depth. The range in each of the cases was 13 m; data were obtained at the same location and time (within 1 hr) as Fig. 4. The PSF was constant with a depth at this location.

only the beam attenuation portion of the curve (a factor of ~0.3 change in on-axis flux). This data set, and others measured at this location, provide an excellent basis for comparison of measurements with the theory of the PSF in a simple environment. We have also made measurements in which variations of the PSF, for a constant range, were evident and will be investigating effects of layered water properties on the PSF.

References

1. See, for example, R. R. Shannon, "The Testing of Complete Objectives," in *Applied Optics and Optical Engineering*, R. Kingslake, Ed. (Academic, New York, 1965), p. 206.
2. See, for example, W. A. Pearce, "Monte Carlo Study of the Atmospheric Spread Function," Appl. Opt. 25, 438–447 (1986).
3. See, for example, J. S. Jaffe and C. Dunn, "A Model-Based Comparison of Underwater Imaging Systems," Proc. Soc. Photo-Opt. Instrum. Eng. 925, 344–350 (1988).
4. L. E. Mertens and F. S. Replogle, Jr., "Use of Point Spread and Beam Spread Functions for Analysis of Imaging Systems in Water," J. Opt. Soc. Am. 67, 1105–1117 (1977).
5. W. H. Wells, "Theory of Small Angle Scattering," in *Optics of the Sea*, AGARD Lecture Series 61 (NATO, 1973).
6. H. C. Van de Hulst, *Light Scattering by Small Particles* (Dover, New York, 1981).
7. A. Morel, "Diffusion de la lumiere par les eaux de mer. Resultats experimentaux et approche theorique," in *Optics of the Sea*, AGARD Lecture Series 61 (NATO, 1973).
8. See, for example, N. W. Witherspoon, *et al.*, "Experimentally Measured MTF's Associated with Imaging Through Turbid Water," Proc. Soc. Photo-Opt. Instrum. Eng. 925, 363–370 (1988).
9. R. C. Honey, "Beam Spread and Point Spread Functions and Their Measurement in the Ocean," Proc. Soc. Photo-Opt. Instrum. Eng. 208, 242–248 (1979).
10. J. E. Tyler and R. C. Smith, *Measurements of Spectral Irradiance Underwater* (Gordon & Breach, New York, 1970), p. 19.
11. R. W. Austin and G. Halikas, "The Index of Refraction of Seawater," SIO Ref. 76-1, Scripps Institution of Oceanography, U. California, San Diego (1976).